Plasma excitation processes in flue gas simulated with Monte Carlo electron dynamics

J. Phys. D: Appl. Phys. **30** (1997) 1636–1645. Printed in the UK PII: S0022-3727(97)75984-9

Plasma excitation processes in flue gas simulated with Monte Carlo electron dynamics

Marnix A Tas, E M van Veldhuizen and W R Rutgers

Division of Electrical Energy Systems, Eindhoven University of Technology, PO Box 513, 5600 MB Eindhoven, The Netherlands

Received 5 July 1996, in final form 5 March 1997

Abstract. The excitation of gas molecules in flue gas by electron impact is calculated with a Monte Carlo (MC) algorithm for electron dynamics in partially ionized gases. The MC algorithm is straightforward for any mixture of molecules for which cross sections are available. Electron drift is simulated in the first case for homogeneous electric fields and in the second case for secondary electrons which are produced by electron-beam irradiation. The electron energy distribution function, $\bar{\varepsilon}_e$, $\bar{v}_d$, $\bar{\lambda}$, the energy branching and the rate of excitation are calculated for standard gas mixtures of Ar–N_2, O_2 and H_2O. These fundamental process parameters are needed for the study of reactions to remove NO_x from flue gas. The calculated results indicate that the production of highly excited molecules in the high electric field of a streamer corona discharge has an efficiency similar to that of electron-beam irradiation.

1. Introduction

Plasma treatment of flue gas to remove NO_x and SO_x is a topic in plasma research. An important aspect is the attempt to reduce the energy costs of the plasma process. An extensive series of experiments with simulated flue gas in a pulsed corona discharge reactor has been performed to elucidate the reaction mechanism of NO_x-removing reactions [1–3]. The subject of this paper is the simulation of fundamental processes occurring in the plasma treatment of the simulated flue gas. Knowledge of fundamental process parameters is needed in order to understand and explain the experimentally observed reactions in plasmas. For this purpose a Monte Carlo algorithm will be used to describe the electron dynamics in partially ionized gases.

Monte Carlo methods are widely used for complex physical and mathematical problems. Examples of Monte Carlo approaches in the field of gas discharges have been given by several authors. The trajectory of electrons in a reactor configuration can be computed by means of a Monte Carlo algorithm [4–8]. The so called 'zero-collision' Monte Carlo method, originally developed by Skullerud [9], is frequently used to compute plasma parameters, see [10–12]. This algorithm, based on collisional frequencies of the electron, is currently mostly used for noble gases. The so-called particle-in-cell method has been applied to RF discharges by Birdsall [13] and Sommeren [14]. The similarity of results obtained by Monte Carlo methods and the numerical solution of the Boltzmann equation was shown by Segur *et al* [15]. They stressed the necessity of using more than the first four terms of the spherical harmonic expansion in the solution of the Boltzmann equation.

Our approach is the simulation of the trajectory of a free electron in a partially ionized gas, using a stochastic process for elastic and inelastic collisions with gas molecules and other free electrons. This Monte Carlo algorithm can be used to simulate the electron dynamics under the influence of a homogeneous electric field or as a result of electron-beam irradiation. In the first case the electrons gain energy from the electric field. In the second case the electrons start with an initial kinetic energy. The electron energy distribution function (EEDF), the drift velocity, the mean electron energy, the branching of the discharge energy and the rate of exciation are obtained by averaging samples from the state of the electron. The computer program named 'Monte Carlo Electron Dynamics' (MCED) developed to perform these calculations can be obtained by contacting the authors. In this paper, a comparison between fundamental processes occurring in different gas mixtures treated by streamer corona plasma and electron-beam irradiation is made.

2. The Monte Carlo algorithm

The gas mixture in which the electron motion is simulated is modelled as a uniform matrix of gas molecules. Each molecule is positioned in a cubic *unit cell* with volume $V_{mol} = 1/n$ and side $\Delta s = V_{mol}^{1/3}$, in which n is the density (in number of molecules per unit volume). The *actual* density is not important since the incorporated two-body

0022-3727/97/111636+10$19.50

interactions scale with the *reduced* field strength E/n. The electron motion from one unit cell to the next under the influence of the electric field is straightforward. Random numbers determine the type of molecule in the next unit cell and whether interaction occurs. The velocity of the molecules is neglected since their mass is more than three orders larger than the electron mass.

2.1. The computational sequence

The basis of the Monte Carlo algorithm used in this paper is a re-definition of the EEDF. Usually, the EEDF is defined as the energy distribution of an assembly of N electrons at time t_1. We state that, under identical conditions, the same EEDF is found when the energy of a *single* electron is sampled at N moments in time. In one respect this approach is better than the conventional one because here the initial energy has to be chosen for one electron only. This energy is taken with a random number from a Boltzmann distribution with an estimated temperature. Its value, however, does not have a great influence since it is lost within a few collisions, which should be compared with the millions of collisions during the simulation. The electron then continues on its way with a realistic energy value. A second and large advantage of this transformation is that the storage of data from a single electron does not require much computer memory. The number of samples from a single simulated electron is limited by computational time only. Furthermore, the algorithm for the simulation of electron drift is less complicated for a single electron than it is for N electrons. The single electron which is simulated by the program is called the *test electron* in the following.

The Monte Carlo algorithm proceeds as follows. First, a uniform random number is generated to determine the type of molecule m for possible interaction with the electron. The probability of finding a molecule of type m, P^m, is equal to the fractional density of this molecule:

$$P^m = \frac{n(m)}{\sum_j n(j)} \tag{1}$$

where $n(m)$ is the partial density of molecules of type m. This procedure allows the simulation of complex gas mixtures without increasing the computational effort. Second, a subsequent uniform random number is used to determine whether the electron will interact. The probability of interaction, $P^i(m,\varepsilon)$, for an electron of energy ε with a molecule of type m is defined as

$$P^i(m,\varepsilon) = \frac{\sigma_{tot}(m,\varepsilon)}{\sigma_{cell}} \ll 1. \tag{2}$$

In this equation $\sigma_{tot}(m,\varepsilon)$ is the total interaction cross section of a molecule of type m at an impact energy ε of the electron and $\sigma_{cell}(=\Delta s^2)$ is the cross section of the unit volume cell within which a matrix molecule is positioned. That the probability of interaction scales with the density of the matrix gas follows directly from the definition of the mean free path $\lambda = 1/(n\sigma)$, which is validated by our scheme [16].

Third, in the case of electron interaction, the second random number is also used to select the specific interaction of the electron with the molecule. The specific interaction is selected from the total interaction cross section $\sigma_{tot}(m,\varepsilon)$, which is the sum of the cross sections for elastic scattering, rotational, vibrational and electronical excitation, attachment, dissociation and ionization of the molecule:

$$\sigma_{tot}(m,\varepsilon) = \sum_k \sigma_k(m,\varepsilon). \tag{3}$$

The specific excitation cross sections $\sigma_k(m,\varepsilon)$ are functions of the electron impact energy ε.

The random numbers which are used in this algorithm are generated by the standard IBM uniform random-number generator RANDU: $x_{n+1} = 65539x_n \pmod{2^{31}}$. The quality of this random-number generator is sufficient for the current simulations because its cycle length is long compared with the total amount of random numbers used in one simulation.

2.2. Homogeneous electric field simulations

In the case of electron drift under the influence of a constant electric field, the test electron is accelerated to the next unit cell over a distance Δs, namely the side of the unit cell. The acceleration of the electron is calculated in the momentum space since it is essential to know the direction of momentum relative to the electric field:

$$\boldsymbol{p}(t+\Delta t) = \boldsymbol{p}(t) + \frac{q\boldsymbol{E}}{m_e}\Delta t \tag{4}$$

with

$$\Delta s^2 = \left[\left(v_\parallel + \frac{qE}{2m_e}\Delta t\right)^2 + v_\perp^2\right]\Delta t^2 \tag{5}$$

where $v_\parallel$ and $v_\perp$ are the velocities of the electron respectively parallel and perpendicular to the electric field $\boldsymbol{E}$ at time t. The value of the residence time Δt of the test electron in a unit cell cannot be obtained analytically from this equation. Therefore, the acceleration of the electron is approximated under two regimes. At a low electron velocity, the acceleration in a unit cell is dominated by the electric field. At a higher electron velocity, the acceleration is relatively small because of the short residence time in the unit cell. The change in momentum of the electron over a distance Δs is approximated by the following scheme:

$$\Delta\tilde{p}_\parallel = \begin{cases} (\Delta s E)^{1/2} & \varepsilon < E\Delta s \\ \Delta s E/(2\tilde{p}) & \varepsilon \geq E\Delta s \end{cases} \tag{6}$$

$$\Delta\tilde{p}_\perp = 0$$

where $\tilde{p} = \sqrt{\varepsilon}$ denotes the momentum in the unit cell used in the program MCED. This approximation represents the trajectory of the electron sufficiently accurately when $|\Delta s||E| \ll 0.1$ eV. Using this criterion for the increment of the electron energy, the gradients and peak values of the cross sections are followed accurately.

2.3. Electron beam simulations

In the case of electron-beam simulations, a large number of electrons is simulated. In this case there is no electric field. Each electron starts with an initial kinetic energy of 200 eV, which corresponds approximately to the energy of secondary electrons produced by the highly energetic primary electron-beam electrons. This method of simulation of electron-beam irradiation requires cross sections for molecules only in the energy range lower than about 300 eV.

The simulation of a secondary electron is continued until all its energy has been transferred to excitation of gas molecules. Subsequently, the possibility newly produced secondary electrons are simulated until they also have lost their energy. Effectively, all the initial energy is transferred to the gas molecules. Many secondary electrons are simulated until statistical convergence has been obtained.

2.4. Other features

Average values of the fundamental plasma parameters EEDF, $\bar{\varepsilon}_e$, $\bar{v}_d$, $\bar{\lambda}$, energy branching and rate of excitation are obtained by averaging many samples of the state of the test electron and its interactions with molecules. More details of the computational Monte Carlo algorithm and the procedure of sampling were described in an earlier publication [1].

3. Electron collision processes

Three classes of electron interactions are implemented in the program MCED: (i) elastic electron–molecule collisions, (ii) inelastic electron–molecule collisions and (iii) electron–electron interaction. These interactions are described below. Super elastic electron–molecule and electron–ion interactions were not implemented since these interactions have minor influences at the E/n values involved.

3.1. Elastic electron–molecule (e–M) collisions

The major effect of elastic electron–neutral species collisions is deflection of the electron. The angle of deflection is derived from the model of scattering from a hard sphere. Owing to the large number of collisions the movement of the electron through the gas is nearly isotropic. As a result the drift velocity in the direction of the electric field is much smaller than the average speed of the electron.

The momentum transfer is small due to the large difference in electron and molecule masses. The energy loss of the test electron is approximated in the program MCED from the maximum possible momentum transfer in the elastic collision of an electron with a molecule of mass M:

$$\Delta\varepsilon = -\varepsilon\frac{4Mm_e}{(M+m_e)^2} \approx -\varepsilon\frac{4m_e}{M}. \tag{7}$$

In this equation m_e is the mass of the electron.

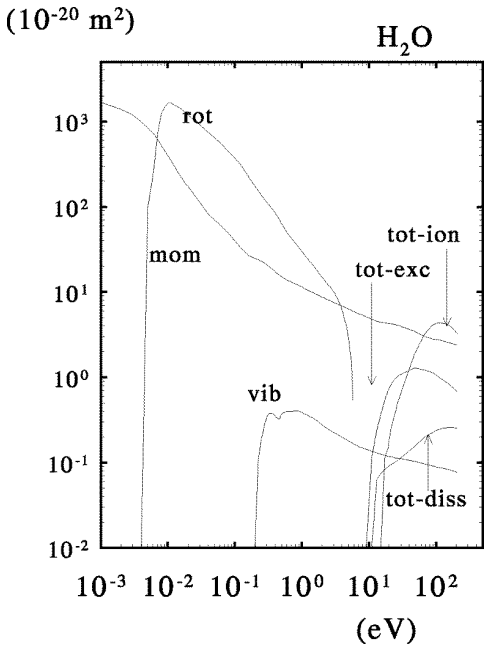

Figure 1. The total cross sections for electron–H_2O interaction as used in our simulations.

3.2. Inelastic electron–molecule (e–M) interactions

Neutral gas molecules can be excited by inelastic electron collisions. Three cases of inelastic collision processes are distinguised in the program.

An *excitation* of a molecule to a uniquely defined state (individual rotations, vibrations and electronically excited states) decreases the energy of the test electron instantaneously with the energy which is required to excite the molecule, ε^{exc}:

$$\Delta\varepsilon = -\varepsilon^{exc} \tag{8}$$

In case of *ionization*, the remaining energy is shared between the test electron and the electron released from the ionized molecule. The energy change of the test electron becomes (the minus sign implies a loss)

$$\Delta\varepsilon = -\varepsilon^{ion} - (\varepsilon - \varepsilon^{ion})rn \tag{9}$$

in which $rn = U[0\ldots1]$ is a uniform random number between 0 and 1. The released electron with energy $(\varepsilon - \varepsilon^{ion})(1 - rn)$ is not considered further in the uniform field calculations. This energy goes to the background electrons and could influence the electron–electron interaction. This interaction will be shown to have a small effect on the results so that this small correction can safely be neglected.

Attachment of the test electron leads to the loss of all its energy:

$$\Delta\varepsilon = -\varepsilon. \tag{10}$$

The simulation is continued with a new test electron with zero kinetic energy.

3.3. Electron–electron (e–e) interactions

The test electron can interact with other free electrons with a Coulomb cross section. The background electrons are

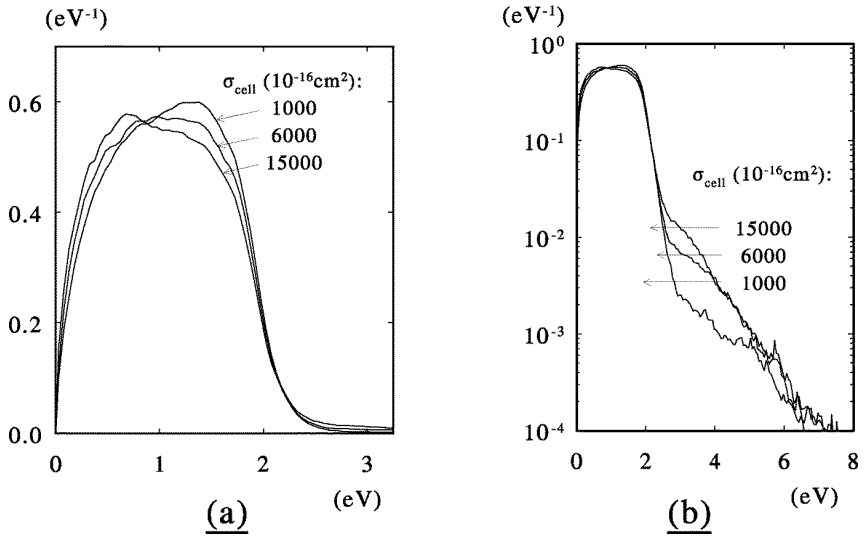

Figure 2. The effect of the size of the unit cell on the EEDF of N_2 at $E/n = 50$ Td and a degree of ionization of 10^{-4}.

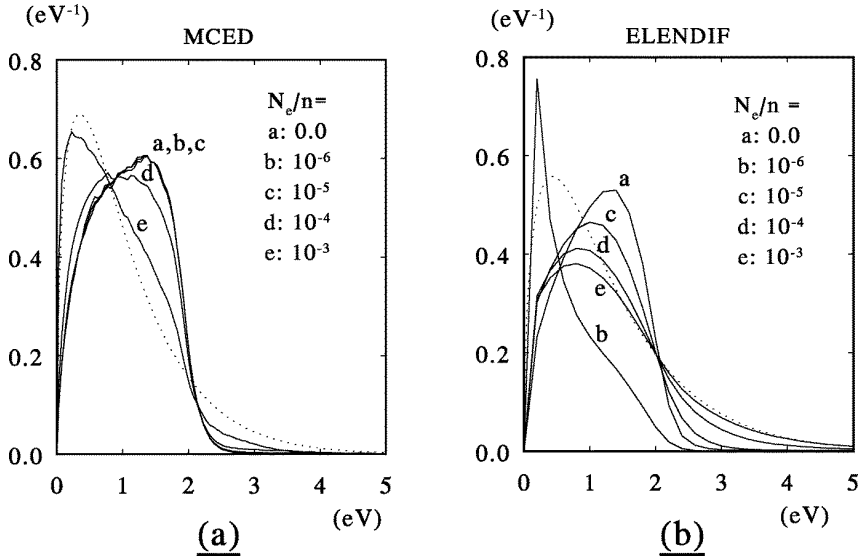

Figure 3. The EEDF of N_2 at $E/n = 50$ Td as a function of the ionization degree. The curves of the EEDF tends towards Maxwellian nature at higher electron density. The dotted lines are Maxwellian distribution functions.

assumed to have an isotropic velocity distribution with a certain background EEDF. In the case of e–e interaction, the energy of the background electron is taken randomly from the background energy distribution function. Currently only two iterations are used for the electron background EEDF. Firstly the EEDF is computed neglecting e–e interaction. In a second iteration, this EEDF is used for the background electrons and the e–e interaction is included. More iterations do not lead to more correct physical results, as will be explained in the discussion below. Furthermore, the simulations described in section 4 will show that including e–e interactions results in relatively small corrections to the physical parameters of interest.

The Coulomb cross section for e–e interaction, $\sigma_c(\varepsilon_{coll})$, was taken from Mitchner and Kruger [17]. The collisional energy, ε_{coll}, was calculated by the scheme of Hashiguchi [5]. The scheme of Hashiguchi assumes an isotropic velocity distribution of the background electrons. This assumption is valid as long as the electrons are in equilibrium with the electric field (the hydrodynamic approximation). Only at very high reduced electric field strengths (>1500 Td) is this assumption violated and will runaway of electrons occur. Such high values of the electric field do not occur in corona discharges.

The energy exchange between the test electron with energy ε_t and the background electron with energy ε_b was performed according to the scheme of Weng and Kushner [11]. These equations can be simplified to

$$\Delta\varepsilon_t = \begin{cases} +\varepsilon_b rn & \varepsilon_t < \varepsilon_b \\ -\varepsilon_t rn & \varepsilon_t \geq \varepsilon_b \end{cases} \qquad (11)$$

where $rn = U[0 \ldots 1]$ is a random number between 0 and 1. This efficient scheme assumes an isotropic background

electron 'fluid' whereby no angle information is included. The net average energy exchange between the test electron and the randomly selected background electrons is zero. This e–e interaction scheme strongly tends to drive the EEDF to Maxwellian behaviour.

The Coulomb cross section becomes very large at low e–e collisional energy. The cross sections for the long-range Coulomb interaction within the Debye sphere can be several orders of magnitude larger than those of the short-range electron–molecule interaction. The Coulomb cross section exceeds the dimensions of the unit cell at a low collisional energy of the free electrons. For example; $\sigma_{cell} \approx 1100 \times 10^{-20}$ m^2 at $p = 10^5$ Pa and $T = 298$ K whereas $\sigma_c > 1100 \times 10^{-20}$ m^2 at $\varepsilon_{coll} < 6$ eV. The size of the unit cell cannot be increased to much larger than $10\,000 \times 10^{-20}$ m^2 since the probability of electron–molecule interaction will become very low in that case and the time of calculation consequently exceedingly long. Therefore, the e–e interaction is slightly underestimated by the program MCED.

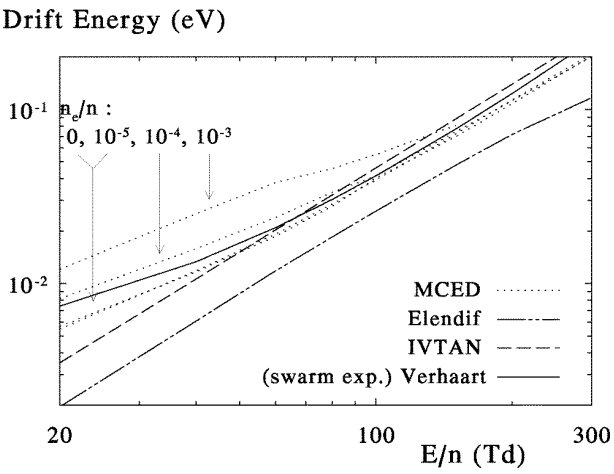

Figure 4. The electron drift energy in dry air in the direction of the E field as a function of the reduced electric field strength E/n. The semi-empirical relation used by IVTAN is $v_e = 3.2 \times 10^3 (E/n)^{0.8}$ m s^{-1} with E/n in Td.

4. A comparison with the literature

The program MCED was tested by comparing the results with data from the literature and with results from the computer program Elendif [18]. The cross sections for O_2 were taken from Eliasson [19]; these for N_2 and Ar from Morgan and Penetrante [18]. These cross sections are well-established ones. The cross sections for H_2O were collected from many references [20–25]. The calculated rotational cross section for H_2O of Itikawa [21] was scaled until the electron drift measurements of Pack *et al* had been reproduced [26]. The cross sections used for H_2O are depicted in figure 1.

Firstly, the electron–neutral species interaction in the program MCED was tested. The e–e interaction was not included in this series of simulations. The energy branching in pure O_2 was calculated as a function of E/n. The MCED result was almost identical to the graph presented in the report of Eliasson [19] from which e–e interaction was also omitted. The only difference is that ionization started later than $E/n = 140$ Td instead of at $E/n = 100$ Td for the results of Eliasson. Furthermore, the EEDFs for dry air (80% N_2 plus 20% O_2) at $E/n = 20$–200 Td were calculated and compared with those calculated by Elendif. The results differ in details only. The peak values of the EEDFs computed by MCED are 10% higher than those from Elendif. This was compensated by a smaller half width. The tails of the distribution functions were almost the same.

Secondly, e–e interactions were included in a series of simulations. The influence of the size of the unit cell and the degree of ionization were determined for N_2 as test gas at $E/n = 50$ Td.

The cross section of the unit cell was increased from 1000×10^{-20} m^2 to $15\,000 \times 10^{-20}$ m^2. The degree of ionization was kept constant at 10^{-4}. The calculated EEDFs changed slightly upon increasing the size of the unit cell (see figure 2). The maximum cross section of the unit cell was about $10\,000 \times 10^{-20}$ m^2 in order to maintain reasonable statistics for electron–molecule interactions during 1 h of simulation on a 40 MHz 486DX computer. Computer time limited the use of our Monte Carlo algorithm to cross sections within a range of four orders of magnitude.

Furthermore, the degree of ionization was varied among the values $0, 10^{-6}, 10^{-5}, 10^{-4}$ and 10^{-3}. The size of the cross section of the unit cell was kept constant at $10\,798 \times 10^{-20}$ m^2. The EEDFs calculated by MCED and Elendif are plotted in figure 3. The e–e interaction results in relatively small corrections to the EEDF calculated by MCED. The Monte Carlo approximation in MCED of the e–e interaction tended to change the EEDF to a Maxwellian one and the mean electron energy did not change, as had been expected.

The results of Elendif are quite different in many respects. The EEDFs calculated by Elendif were changed much more by e–e interaction than were those of MCED. The mean electron energy shifted slightly towards higher values and the tail of the EEDF was populated more. The strange curvature of the EEDF at the degree of ionization 10^{-6} seems to have been caused by a numerical instability in Elendif.

Finally, the average drift energy (defined as $0.5 m_e v_d^2$) of the test electron in the direction of the E field was computed for dry air as a function of the reduced field strength in the range $E/n = 10$–300 Td and the degree of ionization. The calculated drift energy was compared with the computational results of Elendif, the experimental values measured by Verhaart [27] and the semi-empirical relation used by the streamer propagation program IVTAN [28]. The results are plotted in figure 4. The drift energies computed by MCED were much closer to the experimental values than were the results of Elendif. The deviations of Elendif are likely to have been caused by the two-term approximation of the Boltzmann equation. The necessity of using more terms has been stressed by several authors [15, 18, 29]. The results of MCED for degrees of ionization $0, 10^{-5}$ and 10^{-4} were much the same (see also

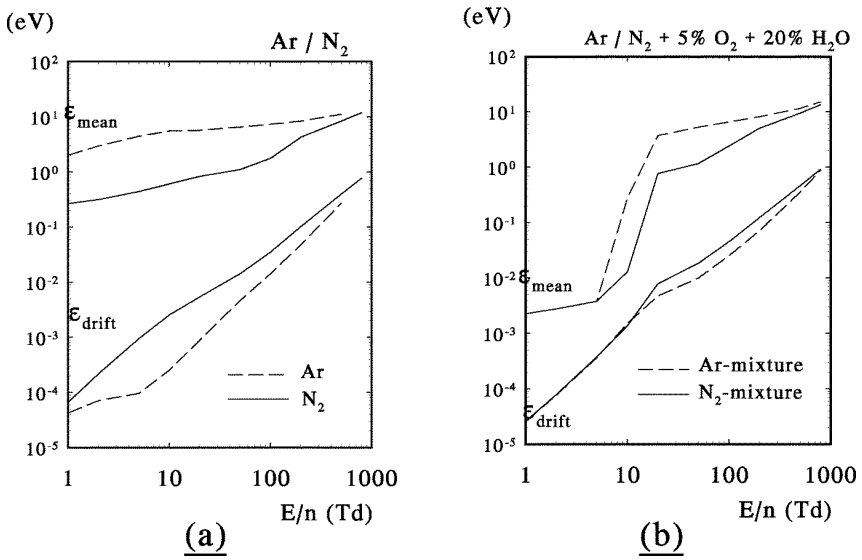

Figure 5. The mean drift and mean electron energy in N_2 and Ar and their mixtures with O_2 and H_2O as functions of the reduced electric field strength E/n.

Table 1. The calculated G values of excited states and ions from the simulation of the secondary electrons from electron-beam irradiation in various gas mixtures. The G value is defined as the number of species produced per 100 eV energy input. The excited states which are taken into counted are: N_2^* and Ar^* at and above their metastable levels and O_2^* and H_2O^* at and above their dissociation levels of 9 and 6 eV respectively.

Electron-beam energy (eV)	N_2	Ar	N_2 with 5% O_2 and 20% H_2O	Ar with 5% O_2 and 20% H_2O
Excited states				
75	5.1	5.5	5.3	6.5
100	5.6	5.6	5.7	6.5
150	5.9	5.6	5.9	6.5
200	5.8	5.7	5.9	6.5
Ions				
75	1.6	3.3	1.7	3.1
100	1.6	3.4	1.8	3.2
150	1.8	3.5	1.9	3.3
200	1.9	3.5	2.1	3.3

figure 3). This shows that e–e interactions do not have much influence at low degrees of ionization. Therefore, the calculations presented in section 5 were performed without e–e interaction.

5. Applications to gas compositions

In research into plasma-induced removal of NO_x and SO_x from flue gas, many gas compositions have been used. There is a great need for standardization of the composition of test gas mixtures in order to allow comparisons among the different methods of plasma treatment.

We performed calculations for the following four gas compositions which we propose as standard mixtures for the study of NO_x removal reactions: (i) N_2, (ii) Ar, (iii) N_2 with 5% O_2 and 20% H_2O and (iv) Ar with 5% O_2 and 20% H_2O. These mixtures with low concentrations of NO pollutant were used in our previous experiments [2, 3]. The plasma in the first two mixtures induces reduction of NO, whereas the plasma in the last two mixtures induces efficient oxidation of NO [2, 3, 30]. The use of Ar instead of N_2 as bulk gas is useful in allowing elucidation of the importance of $N^\bullet$ radicals. The small concentration of NO in the gas mixture is neglected in the simulations since the probability of direct electron impact with NO is very small. NO reacts predominantly with excited species from the bulk gas mixture.

In the results presented below we distinguish between the highly excited species which are chemically active for reaction with NO and the less excited species which are not reactive. The *highly* excited states which are assumed to be chemically reactive were N_2^*, Ar^*, O_2^* and H_2O^*. All species included here have sufficient energy to dissociate water and oxygen (threshold energies of 9 and 6 eV respectively). In practise most of them are in a metastable state. The *less* excited states which are assumed not to be reactive were N_2^*, Ar^*, O_2^* and H_2O^*. The states included here were vibrations, rotations and excitations below 6 eV; in the case of Ar momentum can also be significant.

Simulations both of electron drift in streamer corona and of electron-beam irradiation were performed. Electron

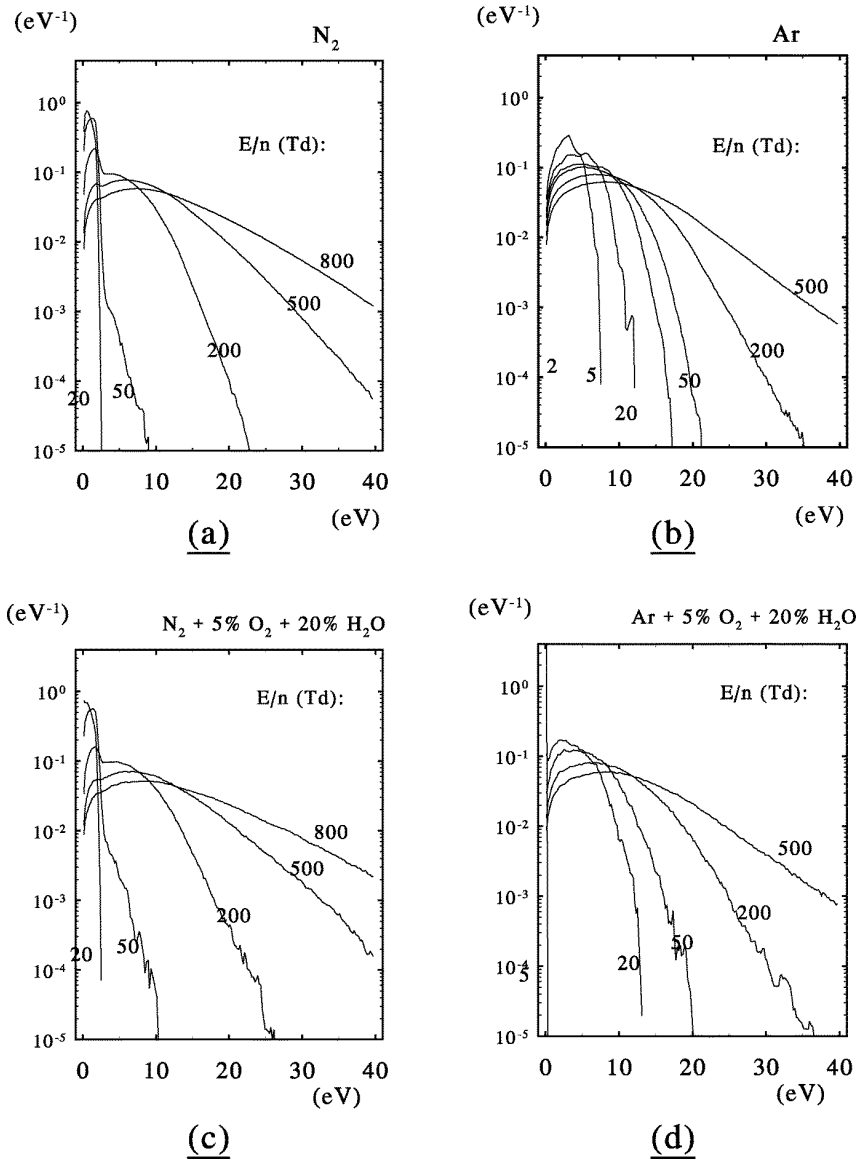

Figure 6. The EEDFs in N_2 and Ar and their mixtures with O_2 and H_2O as functions of the reduced electric field strength E/n.

drift in a homogeneous electric field was used to study the excitation properties in different regions of corona streamers. High values of the electric field, typically $E/n > 500$ Td in air, occur in the propagation head of the streamer. The electric field strength is much lower in the weakly conducting path generated by the streamer head; typically $E/n \ll 50$ Td in air.

The electron-beam simulations were mainly used to determine the energy branching in the gas mixtures. These values can be compared to these of a streamer corona.

5.1. N_2–Ar

The homogeneous electric field simulations with N_2 and Ar gases were performed at $E/n = 1$–800 Td. The calculated drift and mean electron energy are depicted in figure 5. The mean electron energy in Ar was significantly higher than that in N_2, whereas the drift energy of Ar was systematically lower. The lower mean electron energy in N_2 originated from the efficient vibrational excitation of N_2. The latter fact also clearly influenced the EEDF of N_2, see figure 6. The EEDF of N_2 at $E/n \leq 200$ Td was highly non-Maxwellian. There was a large population of electrons with energy below 3 eV. Only at $E/n > 500$ Td did the EEDF become more Maxwellian, especially at higher energies. For Ar, the EEDF was closer to Maxwellian over the whole range of reduced field strengths. The corresponding branching of the discharge energy, figure 7, showed a predominant vibrational excitation of N_2 at $E/n < 400$ Td. The high rate of energy transfer to vibrational excitation of N_2 reduces the maximum transfer of discharge energy to highly excited states to about 70% at $E/n = 800$ Td. Since Ar does not have vibrationally excited states, the discharge energy is transferred almost 100% to excitation of Ar at $E/n > 20$ Td.

The results of the simulation of secondary electrons from electron-beam irradiation, depicted in figure 8, showed that the energy branching in N_2 equalled the branching

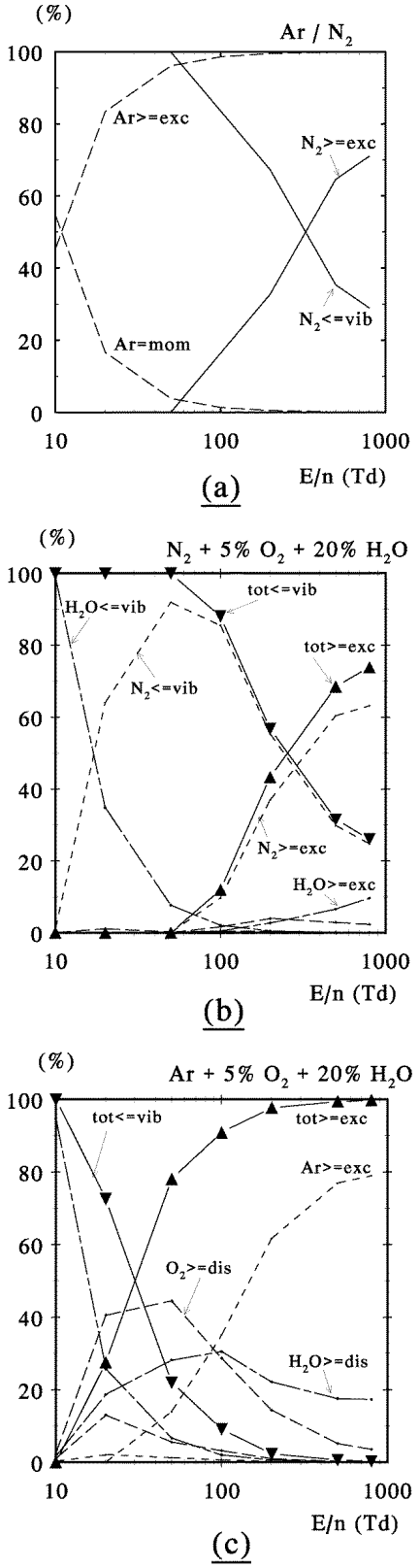

Figure 7. The branchings of the discharge energy in N_2 and Ar and their mixtures with O_2 and H_2O as functions of the reduced electric field strength E/n.

in the streamer head: about 70% of the electron-beam energy was transferred to highly excited states of N_2. The calculated G values for the production of reactive species are presented in table 1.

The electron-beam simulation for Ar, figure 8, showed that the energy transfer to momentum was high, 20%. Since Ar does not have excited states below 11.55 eV, all remaining energy of an electron below 11.55 eV is transferred to momentum excitation.

5.2. N_2–Ar with 5% O_2 and 20% H_2O

The homogeneous electric field and electron-beam simulations were repeated with N_2 and Ar mixtures which contain O_2 and H_2O. The drift and mean electron energy for these mixtures are plotted in figure 5(*b*). The mean electron energy was strongly influenced by the large rotational cross section of H_2O. The mean electron energy remained very low, 10^{-3}–10^{-2} eV, at $E/n \leq 10$ Td. At higher reduced field strengths, a sharp increase in the mean energy was observed because the electrons could overcome the rotational cross section of H_2O [26]. The step was less sharp for N_2 than it was for Ar mixtures since the vibrational excitation of N_2 consumed discharge energy efficiently. The electron drift energy did not differ much for these two mixtures.

The calculated EEDFs for the N_2 and Ar mixtures, figure 6, show the same characteristics as for pure N_2 and Ar gases. However, at low E/n, the EEDF was compressed rapidly to below 1 eV by the large rotational cross section of H_2O. The corresponding branching of the discharge energy is plotted in figure 7. The rotational/vibrational excitation of H_2O dominated the energy transfer at $E/n <$ 40 Td. At higher reduced field strength, the direct energy transfer to H_2O decreased rapidly and the major compound in the mixture was excited predominantly. For the N_2 mixture, a maximum of 75% energy transfer to highly excited states was calculated. Vibrational excitation of N_2 remained an important energy loss mechanism during the acceleration of electrons. For the Ar mixture, almost 100% energy transfer to highly excited states occurred at $E/n \geq 100$ Td.

The energy branching calculated from the electron-beam simulations, figure 8, shows that the efficiency of energy transfer to highly excited species was comparable to that in the case of electron drift in high electric fields. For the N_2 mixture, at most 71% of the electron-beam energy was transferred to chemically active species; for the Ar mixture at most 85% was transferred. The electron-beam energy was mainly transferred to the major constituents of the gas mixtures; N_2 and Ar. The energy transfer to direct dissociation or ionization of H_2O did not exceed 15% in both mixtures. The direct dissociation of O_2 was also inefficient.

6. Conclusions

A Monte Carlo algorithm has been developed to calculate the EEDF, $\bar{\varepsilon}_e$, $\bar{v}_d$, $\bar{\lambda}$, the energy branching and the rate of excitation by electron drift in homogeneous electric fields or electron-beam irradiation. The method used of one electron sampled N times is simple, efficient and can be applied to any mixture of gases. The results are more consistent and

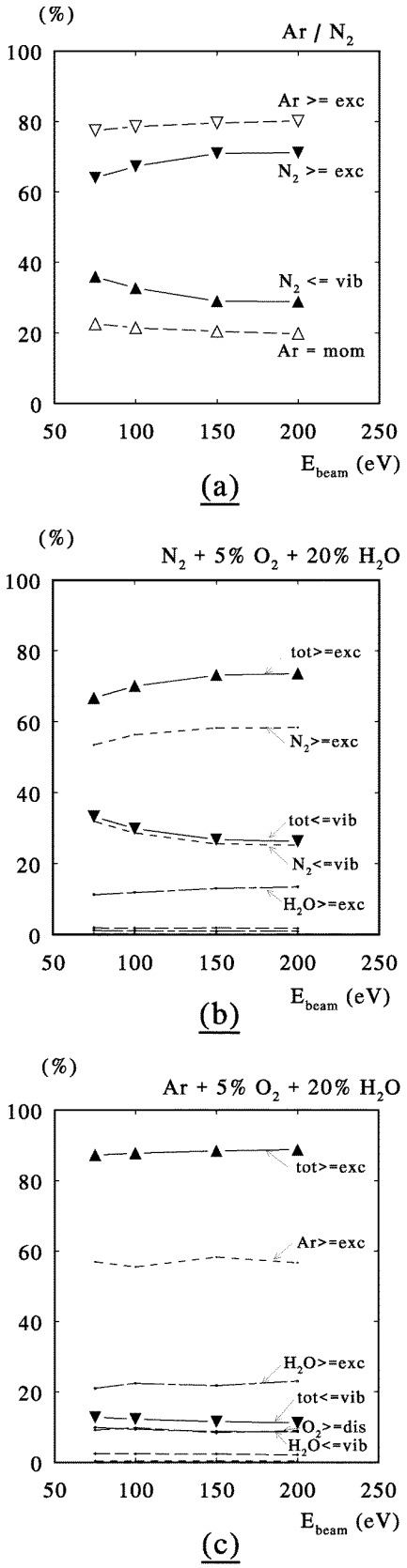

Figure 8. The branchings of the discharge energy in N_2 and Ar and their mixtures with O_2 and H_2O as functions of the initial energy of secondary electrons produced by electron-beam irradiation.

compare better with experimental values than do those of two-term solutions of the Boltzmann equation, as has been shown for the electron drift energy.

The current simulations were performed for pure N_2, pure Ar and their mixtures with O_2 and H_2O. These gas mixtures are proposed as standard mixtures for the study of NO_x removal reactions in plasmas. The calculated branching of the discharge energy shows that the generation of chemically active species by electron-beam irradiation has an efficiency comparable to that under the conditions in the head of the streamer. The dissipation in the tail of the streamer is mainly due to rotational and vibrational excitation of H_2O and N_2. This is probably less effective in chemical processes. Therefore, the importance of very short discharge pulses for the generation of a streamer corona has been stressed by our results.

Acknowledgment

We thank DSM Research, Geleen, The Netherlands, for financial support.

References

[1] Tas M A 1995 Plasma-induced catalysis, a feasibility study and fundamentals *Thesis* Eindhoven University of Technology
[2] van Veldhuizen E M, Rutgers W R and Bityurin V A 1996 Energy efficiency of NO removal by pulsed corona discharges *Plasma Chem. Plasma Processes* **16** 227
[3] Tas M A, van Veldhuizen E M and van Hardeveld R 1997 Reactions of NO in a positive streamer corona plasma *Plasma Chem. Plasma Proc.* at press
[4] Braglia M 1992 *Contrib. Plasma Phys.* **32** 497
[5] Hashiguchi S 1991 *IEEE Trans. Plasma Sci.* **19** 297
[6] Palov A P, Pletnev V V and Tel'kovskii V G 1991 *Sov. J. Plasma Phys.* **17** 295
[7] Satoh K, Ohmori Y, Sakai Y and Tagashira H 1991 *J. Phys. D: Appl. Phys.* **24** 1354
[8] van Veldhuizen E M 1983 The hollow cathode glow discharge analyzed by optogalvanic and other studies *Thesis* Eindhoven University of Technology
[9] Skullerud H R 1968 *J. Phys. D: Appl. Phys.* **1** 1567
[10] Himoudi A and Yousfi M 1992 *Proc. Xth Int. Conf. on Gas Discharges and their Applications Swansea, 13–18 September* vol 2, ed W T Williams (Swansea: University College of Swansea) p 848
[11] Weng Y and Kushner M J 1990 *Phys. Rev.* A **42** 6192
[12] Yousfi M, Himoudi A and Gaouar A 1992 *Phys. Rev.* A **46** 7889
[13] Birdsall C K 1991 *IEEE Trans. Plasma Sci.* **19** 65
[14] Sommeren T J 1993 *Plasma Sources Sci. Technol.* **2** 198
[15] Segur P, Yousfi M and Bordage M C 1984 *J. Phys. D: Appl. Phys.* **17** 2199
[16] Kittel C and Kroemer H 1980 *Thermal Physics* 2nd edn (New York: Freeman)
[17] Mitchner M and Kruger C H Jr 1973 *Partially Ionized Gases* (New York: Wiley)
[18] Morgan W L and Penetrante B M 1990 Elendif 93: the Boltzmann equation solver *Comput. Phys. Commun.* **58** 127
[19] Eliasson B and Kogelschatz U 1986 Basic data for modeling of electrical discharges; ABB Forschungsbericht June 1986
[20] Itikawa Y 1974 *J. Phys. Soc. Japan* **36** 1127
[21] Itikawa Y 1972 *J. Phys. Soc. Japan* **32** 217

[22] Jain A and Thompson D G 1983 *J. Phys. B: At. Mol. Phys.* **16** 3077
[23] Melton C E 1972 *J. Phys. Chem.* **57** 4218
[24] Orient J O and Srivastava S K 1987 *J. Phys. B: At. Mol. Phys.* **20** 3923
[25] Yousfi M, Poinsignon A and Hamadi A 1992 *Phys. Rev.* A **46** 7889
[26] Pack J L, Voshall R E and Phelps A V 1962 *Phys. Rev.* **127** 2084
[27] Verhaart H F A 1989 *Kema Scient. Tech. Rep.* **7** 377
[28] Babaeva N Yu, Kulilovski A A, Mnatsakanyan A Kh, Naidis G V and Solosolov M.Yu 1993 The streamer propagation models in N_2–O_2 mixtures and flue gas, research report IVTAN–ANRA 93/2, Moscow, Russia
[29] Eizenkiet H J and Friedland L 1989 *Phys. Rev.* A **39** 3541
[30] Tokunaga O, Nishimura K, Suzuki N and Washino M 1978 *Radiat. Phys. Chem.* **11** 117